

# A Perspective on Topographic Correction Methods on Satellite Images

Hwee San Lim<sup>1\*</sup>, Eng Choon Yeap<sup>1</sup>, Mohd. Zubir Mat Jafri<sup>1</sup> and Jasim Rajab<sup>2</sup>

<sup>1</sup>School of Physic, 11800 Universiti Sains Malaysia, Penang, Malaysia.

<sup>2</sup>Mustansiriyah University, College of Science, Department of Atmospheric Science, Baghdad, Iraq.

\*Corresponding Author: hslim@usm.my

---

**Abstract** – The presence of atmospheric and topographic effects in satellite images is inevitable, which may reduce image information content. A standard procedure for improving satellite images is topographic and atmospheric correction during preprocessing. The topographic effect on satellite images is not an error but a distortion caused by solar and surface geometries. Surfaces facing toward the Sun tend to be bright, whereas surfaces facing away from the Sun are usually dark. This effect is strongly related to the solar surface incident angle, and it is one of the main factors that increases the spectral variation in satellite images. The objective of this paper is to review the commonly available methods for topographic correction. The spectral variation may reduce the accuracy of processes, such as surface topographical classification, which can limit the capability of autonomous remote sensing applications. Many have tried to reduce the effect of topography and achieved great success; however, most methods are complicated and require many parameters. The topographic correction methods can be categorized into two groups: empirical and physical methods. In this paper, a total of six empirical methods were reviewed, including Cosine correction (CC), Statistical-Empirical (SE) correction, Minnaert (MIN) correction, Shepherd and Dymond's (SD) Correction Method, Sun-canopy-sensor (SCS) Models and Path Length Correction (PLC) Method. The algorithms and models used in the physical topographical correction method were also discussed. Parameters related to the topographic correction algorithm were reviewed in detail. This paper reviewed a total of six common topographic correction methods and seven assessment methods for topographic correction.

**Keywords** –Surface Topography; Topographic Correction; sun-canopy-sensor (SCS); MIN correction.

©2024 Penerbit UTM Press. All rights reserved.

*Article History: Received 10 July 2024, Accepted 1 August 2024, Published 31 August 2024*

*How to cite: Hwee San Lim, Eng Choon Yeap, Mohd. Zubir Mat Jafri and Jasim Rajab (2024). A Perspective on Topographic Correction Methods on Satellite Images. Journal of Advanced Geospatial Science and Technology. 4(2),231-254.*

## 1.0 Introduction

The process of topographic correction involves removing part of the information from satellite images to improve the topographic variation caused by surface and solar geometry (Dong, et al., 2020). This results in some reduction of information in the satellite images. Topographic correction affects the brightness of slopes facing the sun, which will decrease, while those facing away from the sun will increase in brightness after correction (Yin, et al., 2022). As topographic correction affects each pixel in the image differently, it also reduces the radiometric quality. When a shaded surface is brought to light in the correction process, the digital number in that particular pixel is multiplied by a factor calculated by the algorithm that normalizes the dark surface to its surroundings. However, this factor also reduces the radiometric resolution of the pixel, resulting in a relatively lower signal-to-noise ratio and increasing the probability of salt and pepper effects in the shaded area.

The uneven solar illumination is a natural phenomenon that is caused by the uncertainty of surface elevation. In the technical term, uneven solar illumination is due to the changes in solar incident angle on the surface toward the Sun, which is described as topographic distortion in remote sensing images. This unevenness allows us to create a perception of the third dimension from a two-dimensional image (Wallach and O'connell, 1953). In computer vision, this condition may cause problems in the interpretation process and affect the accuracy.

In accordance with previous studies, topographic correction methods can be categorized into two groups: empirical and physical methods (Yin *et al.* 2018). Empirical methods, such as cosine correction (CC) by (Teillet *et al.* 1982), sun-canopy-sensor with diffuse effect correction (SCS+C) by Soenen *et al.* (2005), statistical-empirical (SE) by Teillet *et al.* (1982), and Minnaert (MIN) correction by Minnaert, (1941) do not require much ancillary data by Sola *et al.* (2016). The procedure is easy to implement due to its simplicity. However, the output of empirical methods does not have any physical meaning, which limits its application (Blesius and Weirich, 2005). Gao and Zhang (2009) used data from Landsat-7 Enhanced Thematic Mapper Plus (ETM+) images for topographic correction. In addition, Vanonckelen et al. (2017) examined the effect of topographic correction on land cover classification accuracy, while Federico et al. (2022) investigated the influence of topographic correction on the analysis of vegetation indices. Besides, Dong et al. (2020) and Yin et al. (2022) used Landsat data in their studies to improve the accuracy of forest tree species classification.

Physical methods, on the contrary, consider the propagation of solar irradiance from the atmosphere top to the ground and reflect to sensors along with other radiance, such as atmospheric scattered radiance and multisurface reflectance. They employ a radiative transfer model to calculate the energy arriving at the Earth's surface and apply the cosine law to calculate the surface incident angle (Huang *et al.* 2008). Using a physical model avoids the need for empirical parameters thus achieving high consistency and can overcome the overcorrection problem in cosine and sun-canopy-sensor (SCS) models (Shepherd and Dymond, 2003).

Many attempts have been made in the past to reduce the impact of topography with great success, but most methods are complex and require numerous parameters. To address this issue, the objective of this review paper was to review the commonly available methods for topographic correction that can quantify, reduce, and induce topographical effects on satellite images by exploring the relationship between direct and diffuse solar irradiance.

Multi-temporal studies in remote sensing require images to be homogenized in radiometric and geometric terms to better identify changes in the images. Topographic correction is one of the essential steps in creating radiometrically stable time series satellite images (Hantson and Chuvieco, 2011). Compared to the large number of atmospheric correction algorithms, relatively little attention has been given to correcting topographic illumination.

Topographic distortion is a complex problem in remote sensing because of its irregular nature, as noted by Fan *et al.* (2018). Topographic effects occur naturally and are inevitable. When the sun shines on the Earth's irregular surface, areas facing towards the sun appear brighter, while areas facing away from the sun appear dimmer. Changes in solar intensity are due to changes in the surface solar incident angle. The position of the sun is not constant due to the Earth's orbit, which increases the complexity of solar geometry calculations. This study identified four main problems with topographic distortion: (1) each satellite image is affected uniquely by topography, (2) the topographic effect can impact the accuracy of satellite images, (3) existing physical topographic correction algorithms require many parameters that may be unavailable, and (4) topographic correction can remove part of the information in satellite images in addition to reducing the topographic effect.

In section 1, the background of the study is introduced, followed by a discussion of the problem that motivated the study. The objectives of the study are also presented, along with an explanation of the significance and scope of the research.

Section 2 begins with a review of commonly available topographic correction methods, including a discussion of the algorithm and model used in physical topographic correction. The section also discusses common assessment methods used in topographic correction, as well as parameters related to the topographic correction algorithm. Section 3 provides a detailed description of the assessment methods used in the study for topographic correction. Section 4 contains two case studies conducted as part of the review paper. Finally, section 5 presents a summary of the review paper.

## 2.0 Methodology

The six most common topographic correction methods, which are the CC, SE, MIN correction, SCS, Shepherd and Dymond's (SD), and path length correction (PLC) methods, are discussed in this paper. The topographic correction methods can be categorized into two groups: empirical and physical methods. In this paper, a total of six empirical methods were reviewed, including Cosine correction (CC), Statistical-Empirical (SE) correction, Minnaert (MIN) correction, Shepherd and Dymond's (SD) Correction Method, Sun-canopy-sensor (SCS) Models and Path Length Correction (PLC) Method. Table 1 shows the methods discussed along with their expressions. Some topographic correction methods have been made available in the past few decades. However, the performance of topographic correction methods was not standardized. From the literature, the evaluation methods used to evaluate topographic correction methods are different, unstandardized are hardly comparable (Hantson and Chuvieco, 2011 and Sola *et al.* 2016). Study areas are also different with diverse land cover, topography and solar geometry, which have a direct impact on the magnitude of the reduction of the topographic effect. In accordance with Hantson and Chuvieco, (2011), before 2011, most of the topographic correction methods were not rigorously evaluated because studies only considered images with good illumination conditions and the impact of land covers was not commonly assessed. The first study that addressed this problem was Richter *et al.* (2009), which evaluated different topographic effects with various land covers. Nevertheless, the study images were taken under favorable illumination conditions, which naturally produced enhanced results and did not fully exhibit the full potential of topographic correction methods.

In Hantson and Chuvieco, (2011), the authors used 8 topographic correction methods to improve 15 Landsat ETM images topographically and assessed them with 2 assessment procedures. The topographic correction methods involved in this study were CC, empirical-statistical, empirical-

statistical\_NDVI, C-correction, C-correction\_NDVI, MIN with slope, MIN with slope\_NDVI, and a modified MIN. Fifteen Landsat images at the central part of the Iberian Peninsula with different solar geometries were topographically improved, which returned 120 results. The methods used to assess these results were (1) calculating the changes in the standard deviation of pixel value from the same land cover over different slopes and aspects and (2) measuring the temporal stability of a time series at individual pixels. The results indicated that empirical-statistical method and C-correction produced the best results in terms of the homogeneity of different land covers. In terms of temporal stability, the proof of the empirical-statistical was superior to those of the other methods. However, a good result was only possible when the necessary parameters were estimated independently for each land cover (Gao *et al.* 2016). As a result, artifacts were formed at the border of the land covers. The two main reasons for the formation of the artifacts are

- (1) the large number of mixed pixels and
- (2) the application of different parameter to each land cover,

which caused discontinuity among the classes of land covers (Hantson and Chuvieco, 2011). To improve the topographic correction, a better resolution of digital elevation model (DEM) with topographical match with satellite images and better separation of land covers are necessary.

Table 1. Summary of The Discussed Topographic Correction Methods.

Topographic correction methods	Expression	Author
Cosine correction (CC)	$L_c = L(\cos a / \cos \theta)$	Teillet <i>et al.</i> (1982)
Civco's method	$L_c = L + L(\cos \phi - \cos \theta) / \cos \phi$	Civco, (1989)
C-correction	$L_{c\lambda} = L_\lambda[(\cos iz - C_\lambda) / (\cos \theta - C_\lambda)]$	Teillet <i>et al.</i> (1982)
Statistical-empirical (SE)	$L_{c\lambda} = L_\lambda - (a \cos \theta + b_\lambda) + \bar{L}_\lambda$	Teillet <i>et al.</i> (1982)
Minnaert (MIN) correction	$L_{c\lambda} = L_\lambda \left( \frac{\cos iz}{\cos \theta} \right)^M$	Minnaert, (1941)
Dymond's correction (SD)	$L = \frac{\rho_h^{dir} E^{dir} / \gamma + \rho_h^{dif} E^{dif}}{\pi}$	Shepherd and Dymond, (2003)

sun-canopy-sensor (SCS)	$L_c = \frac{L(\cos \alpha \cos iz)}{\cos \theta}$	Shepherd and Dymond, (2003)
sun-canopy-sensor with diffuse effect correction (SCS+C)	$L_c = \frac{L(\cos \alpha)(\cos iz)}{\cos \theta + C}$	Shepherd and Dymond, (2003)
Path length correction (PLC)	$\rho_{PLC} = \rho_t \frac{S(\Omega_1) + S(\Omega_2)}{S_t(\Omega_1) + S_t(\Omega_2)}$	Yin <i>et al.</i> (2018)

---

## 2.1 Cosine correction (CC)

One of the pioneers and widely discussed topographic correction methods is the CC method (Hantson and Chuvieco, 2011) and Sola *et al.* 2016), which can be expressed in Equation (1),

$$L_c = L(\cos \alpha / \cos \theta) \quad (1)$$

Where:  $L_c$  is the corrected radiance.

$L$  is the reflected radiance of the terrain.

$\alpha$  is the slope angle.

$\theta$  is the incident angle.

This algorithm is easy to apply due to its simplicity and does not require any external parameter. However, it ignores the contribution of diffuse irradiance (Yin *et al.* 2018) and has been reported to present overcorrection under poor illumination (Hantson and Chuvieco, 2011), Huang *et al.* 2008 and Shepherd and Dymond, 2003)]. A few alternative approaches were introduced after CC. One of the new algorithms is that proposed by Civco, (1989) in Equation (2), which considers the average illumination in the calculation.

$$L_c = L + L(\cos \varnothing - \cos \theta) / \cos \bar{\varnothing} \quad (2)$$

Where:  $\bar{\varnothing}$  is the mean illumination angle.

CC and the method proposed by Civco (1989) are wavelength independent, which do not consider diffuse irradiance. To account for the transmission of different wavelengths and diffuse irradiance, C-correction was proposed. C-correction uses  $C_\lambda$  as the wavelength-dependent empirical constant to account for diffuse irradiance (Equation 3).

$$L_{c\lambda} = L_\lambda[(\cos iz - C_\lambda)/(\cos \theta - C_\lambda)] \quad (3)$$

Where:  $iz$  is the incoming solar zenith angle.

$C_\lambda$  is a wavelength-dependent empirical constant, which can be calculated using Equation (4).

$$C_\lambda = B_\lambda/m_\lambda \quad (4)$$

Where:  $B_\lambda$  and  $m_\lambda$  are the regression coefficients of band reflectance and illumination.

## 2.2. Statistical-Empirical (SE) correction

The SE method is one of the empirical methods that do not require much ancillary data. It assumes that radiance varies due to the topography proportional to all wavelengths (Sola *et al.* 2016) (Equation 5).

$$L_{c\lambda} = L_\lambda - (a \cos \theta + b_\lambda) + \overline{L}_\lambda \quad (5)$$

Where:  $b_\lambda$  is the exponent of diffuse sky irradiance

$\overline{L}_\lambda$  is the mean radiance of the image for band  $\lambda$ .

## 2.3. Minnaert (MIN) correction

One of the most cited topographic corrections on non-Lambertian reflection is the Minnaert correction (Minnaert, 1941). In Equation (6), Minnaert constant,  $\mathcal{M}$  is used to present the weight of anisotropic reflectance (Minnaert, 1941 and Bishop and Colby, 2002).

$$L_{c\lambda} = L_\lambda \left( \frac{\cos iz}{\cos \theta} \right)^\mathcal{M} \quad (6)$$

Owing to the dependency of MIN constant on wavelength, land cover type, phase angle and training samples are required for statistical regression to derive each MIN constant (Gao *et al.* 2016). The MIN constant has a value between 0 and 1 with 1 being the perfect Lambertian reflector.

Further improvement of the MIN method includes the method proposed by Bishop and Colby, (2002), which includes slope angle in the calculation, and the method proposed by Gao *et al.* (2016), namely, MIN-E which includes the effect of sky isotropic scattering. In accordance with other research, the performance of MIN-E is considerably better than that of its predecessor (Gao *et al.* 2016).

One of the disadvantages of this approach is the fact that MIN constant is land cover and wavelength dependent, which should be determined separately. This condition increases the complication of the application since land-cover maps are often unavailable (Hantson and Chuvieco, 2011).

#### 2.4. Shepherd and Dymond's (SD) Correction Method

SD is a new physical method, that considers the bidirectional reflectance distribution function (BRDF) in reducing the topographic effect, which is different from previously discussed methods (Shepherd and Dymond, 2003). This physical method requires a radiative transfer model to estimate the direct and diffuse irradiance on a surface. Sun angle and viewing geometries are explicitly involved in the calculation. The general equation for describing the observed brightness is expressed in Equation (7).

$$L = \frac{(\rho_h^{\text{dir}} E^{\text{dir}}/\gamma) + (\rho_h^{\text{dif}} E^{\text{dif}})}{\pi} \quad (7)$$

Where:  $\rho_h^{\text{dir}}$  is the surface reflectance for direct irradiance.

$\rho_h^{\text{dif}}$  is the surface reflectance for diffuse irradiance.

$E^{\text{dir}}$  is the direct solar irradiance on a horizontal surface.

$E^{\text{dif}}$  is the diffuse solar irradiance on a horizontal surface.

$\gamma$  is the relationship between sloping and horizontal surfaces.

The proposed method first estimates the direct and diffuse irradiance on a horizontal surface by using Second Simulation of the Satellite signal in the Solar Spectrum (6S). Afterward, DEM is used to calculate the incident angle for a sloping surface, followed by a cast shadow algorithm that is used with the known solar position to produce a binary shadow mask. The author also added a sky-viewing factor (V) in the calculation to improve the estimation of the contribution from diffuse irradiance. The value of V can be calculated using Equation (8), where  $s$  is the slope angle.

$$V = \frac{1 + \cos s}{2} \quad (8)$$

However, the canopy structure is not accounted for in this method, which causes unsatisfactory topological correction in some cases (Yin *et al.* 2018 and Richter *et al.* 2009). As suggested by Yin *et al.* (2018), the SD method is suitable for isotropy land cover, that focuses on relative accuracy rather than biophysical parameter retrieval that focuses on high absolute reflectance accuracy.

## 2.5. Sun-canopy-sensor (SCS) Models

Most of the topographic correction methods discussed previously did not consider bidirectional reflectance distribution function (BRDF). One popular method to account for BRDF is the use of the SCS correction, which is also a pioneering method in BRDF correction (Yin *et al.* 2018). The expression of SCS is shown in Equation (9). This method assumes that the main contribution factor of pixel reflectance is from sunlit canopy (Yin *et al.* 2018). Similar to CC, pixels with large incident angles over slopes facing away from the Sun are probably overcorrected (Huang *et al.* (2008).

$$L_c = \frac{L(\cos \alpha \cos iz)}{\cos \theta} \quad (9)$$

One of the important disadvantages mentioned by Yin *et al.* (2018) is that SCS correction does not consider the viewing angle effect. This condition may limit its application with a narrow viewing angle. To improve the performance of the SCS correction, a semi-empirical parameter, C, was introduced to account for diffuse irradiance and reduce the overcorrection phenomenon, namely, SCS+C (Equation 10) (Soenen *et al.* 2005). Similar to the previous MIN constant ( $\mathcal{M}$ ), C is a scene-dependent parameter. Although many studies have adopted this method and achieved good results (Thompson *et al.* 2018 and Qiu *et al.* 2019), SCS with improved C correction is a semi-empirical method that is unsuitable for multitemporal and multisensory comparison (Huang *et al.* 2008).

$$L_c = \frac{L(\cos \alpha)(\cos iz)}{\cos \theta + C} \quad (10)$$

## 2.6. Path Length Correction (PLC) Method

A path length is defined as the distance between the top and the bottom of the canopy along with a direction relative to the canopy height (Luisa *et al.* 2008). It is a critical variable that affects the radiative transfer within a canopy (Yin *et al.* 2018) and has been applied to characterize three-dimensional canopy structures for leaf area index (Yan *et al.* 2016) and Hu *et al.* 2018). The path length stretches in the upslope direction while compresses in the downslope direction, which is a major factor causing BRDF distortion (Yin *et al.* 2018).

The derivation of PLC consists of two major steps (Yin *et al.* 2018). The first step is to simplify a radiative transfer equation on the basis of a few assumptions. The first assumption is that the

canopy is illuminated only by collimated light while diffuse and surrounding reflected radiation is negligible. The second assumption is that the radiance collected by a sensor is only from single scattering of leaves while the reflectance from soil and multiple scattering is ignored.

The second step in PLC is to devise a path length over horizontal and sloping terrain. Corrected reflectance can be obtained by substituting the calculated path length from the second step. The simplified expression of PLC on a horizontal surface is shown in Equation (11).

$$\rho_{PLC} = \rho_t \frac{S(\Omega_1)+S(\Omega_2)}{S_t(\Omega_1)+S_t(\Omega_2)} \quad (11)$$

Where:  $\rho_{PLC}$  is the corrected image.

$\rho_t$  is the image-observed reflectance.

$S(\Omega_1)$  is the path length along the solar direction over flat terrain.

$S(\Omega_2)$  is the path length along the viewing direction over flat terrain.

$S_t(\Omega_1)$  and  $S_t(\Omega_2)$  are the counterparts of  $S(\Omega_1)$  and  $S(\Omega_2)$  respectively, over sloping terrain.

The PLC method has been tested against some topographic correction methods on Landsat 8 OLI images with results similar to those for an empirical parameter-based method (Yin *et al.* 2018). In summary, this correction method provides an efficient way to improve terrain-induced canopy BRDF distortion and realize good results, especially over mountainous areas. However, this approach is only suitable for forested land cover. A good understanding of land cover is required for estimating the path length in every image that will complicate the correction process.

### 3.0 Assessment methods for topographic correction

In this review paper, six common topographic correction methods are discussed, along with seven evaluation methods. Additionally, the model and algorithm used in the physical modelling correction method are explained in detail. These include a digital elevation model, an extraterrestrial irradiance model, the calculation of a radiative transfer function, the distribution of solar irradiance on a rugged surface, a bidirectional reflectance distribution function (BDRF), and the conversion of a digital number to surface radiance.

This section is divided into three parts. The first section reviews the available topographic correction methods. The second section explains the algorithm and model used in this study. Finally, the last section discusses the assessment of the correction method. Mishra *et al.* (2017)

presented four methods to assess a topographic correction method, namely the Cosine law, C-correction, Minnaert methods, and Slope-matching method.

Sola *et al.* (2016) presented eight possible ways to assess a topographic correction method. They used 10 topographic correction methods to improve several SPOT images. The correction methods were C-correction, smoothed C-correction, SCS+C, MIN, modified MIN, pixel-based MIN, enhanced MIN, SE, slope matching, and two-stages normalization. In this paper, seven evaluation methods will be discussed. They are

- (1) visual inspection,
- (2) incident angle correlation,
- (3) reduction of land cover variability,
- (4) classification accuracy,
- (5) calculation of the difference between north- and south- facing land covers,
- (6) presence of outliers and
- (7) intraclass interquartile range reduction.

### ***3.1 Visual inspection***

Visual inspection is generally the first indicator of the quality of topographic correction (Shepherd *et al.* 2014). However, evaluating results via vision inspection is impractical because it does not return any quantitative results and it will vary from people to people. This evaluation method has been used by many authors (Yin *et al.* 2018, Sola *et al.* 2016 and Gao *et al.* 2014) in assessing the performance of topographic correction. In Gao *et al.* (2014), topographic correction methods (MIN, MIN+E, SCS+C, and C-HuangWei correction) shows positive results which indicted the reduction of the topographic effect visually. The author mentioned that methods based on the assumption of non-Lambertian reflectance performed better with MIN-E outperforming the others.

### ***3.2. Incident angle correlation***

Incident angle correlation is one of the most used quantitative evaluation methods in assessing topographic correction methods (Yin *et al.* 2018 and Sola *et al.* 2016). Owing to the effect of topography, a significant correlation improvement can be observed after topographic correction (Yin *et al.* 2018), especially for a long wavelength due to the reduction of atmospheric scattering.

The incident angle correlation method is based on the dependency between solar incident angle and the reflected radiance after the correction. The dependency can be measured through a decrease in correlation coefficient (Gao *et al.* 2014). A lower dependency between radiance and incident angle theoretically indicates a better topographic correction. However, this is not always the case. In some areas, slope and aspect influence land cover distribution. In such areas, the correlation between solar incident angle and radiance should be expected after topographic correction (Sola *et al.* 2016).

Several studies in the past used this method in comparing the effectiveness of different topographic correction methods (Yin *et al.* 2018 and Sola *et al.* 2016). A comparison of topographic correction methods by using this evaluation method has shown that PLC, SCS, DS, CC, empirical-statistical method, and SCS+C can reduce the correlation between reflected radiance and incident angle (Sola *et al.* 2016).

### ***3.3. Reduction of land cover various variability***

In theory, the land cover homogeneity should increase after topographic correction (Sola *et al.* (2016). The assessment can be performed by using the standard deviation within each land cover class (Gao *et al.* 2014). This assessment method requires prior knowledge of the land cover distribution and is affected by the land cover accuracy.

Several studies have used this method in assessing the results of topographic correction methods. In Hantson and Chuvieco, (2011), the assessment showed that CC and the empirical-statistical method exhibited the best performance when assessing with this method. Studies conducted by other researchers also acquired the similar results with this assessment method (Sola *et al.* 2016 and Gao *et al.* 2014).

### ***3.4. Classification accuracy***

The topographic effect influences the accuracy of classification due to the uneven distribution of solar irradiance over land surface from this statement, a topographic corrected image is expected to yield a better classification result compared with uncorrected images.

In Huang *et al.* (2008), classification assessment was used to determine the effectiveness of the SCS method. The assessment results showed that the accuracy of classification results was improved from 85% to 89%; particularly, a forest facing away that was previously misclassified

was improved. The author mentioned that the SCS method effectively improved the classification results, especially in forest and woodland that grow on slopes because they have a high tendency to have high spectral confusion.

Some authors may find this method effective, while others may argue that this assessment may entail uncertainties in the classification procedure, which makes it difficult to relate their results to the effectiveness of topographic correction methods (Sola *et al.* 2014 and Hoshikawa and Umezaki, 2014).

### ***3.5. Calculation of the difference between north- and south-facing land covers***

Another method for evaluating the effectiveness of topographic correction is to compare the reflectance from shaded and sunlit areas (Notarnicola *et al.* 2014 and Fan *et al.* 2014). Ideally, topographic correction would reduce the difference between shaded and sunlit samples, increasing the homogeneity in the areas.

Some studies have shown that the difference between sunlit and shaded areas in conifer forests increases along with the topographical effect (Sola *et al.* 2016). Most topographic correction methods can reduce this difference, and some reduce this difference excessively, which shows a negative difference value “A negative value indicates that is image is overcorrected”. Here, the modified MIN method shows a significant overcorrection when assess with this evaluation method, that is, the pixels from a shaded area have much higher radiance than those from a sunlit area after the correction. Other topographical correction methods such as SCS+C, two-stage normalization, and pixel-based MIN show acceptable results with some inconsistency, whereas slope matching and the SE method are the most successful in this assessment (Sola *et al.* 2016).

### ***3.6. Presence of outliers***

Outliers are caused by pixels that are weakly illuminated. When a topographic correction method fails at correcting those pixels, it may result in an abnormally low or high value from the pixels, also known as outliers. An outlier, as defined by Balthazar *et al.* (2012) is a pixel with a value that falls beyond the expected threshold.

In previous studies, the problematic pixels on weakly illuminated area were usually excluded from the evaluation. Some authors suggested that those extreme pixels should be left uncorrected.

However, a good topographic correction method should always return minimal outliers hence, the proportion of statistical outliers should be evaluated than ignored.

In Sola *et al.* (2016), the percentage of outliers on a high solar elevation angle was lower than that on a low elevation angle. The smoothed CC method in this case returned the least outlier compared with other topographic correction methods.

### ***3.7. Intraclass interquartile range reduction***

In theory, reflectance from the same land cover should exhibit spectral signature with a small variance. Owing to the inhomogeneity of solar illumination, the variance of reflectance retrieved from uncorrected images is relatively larger than that from corrected images. With the uncertainty of total surface irradiance, topographic correction may reduce the radiance range. Hence, the reduction of intraclass variance can be measured using statistical measurement as a method of assessment of the effectiveness of topographic correction.

The drawback of this assessment method is that the presence of outliers during topographic correction could affect the results of the study (Sola *et al.* 2016)]. This effect can be reduced if the interquartile range is measured due to minimal sensitivity to outliers.

The reduction of intraclass interquartile range depends on the amount of topographic effect that is present in an image. An image with a high topographic effect is expected to have a large interquartile range. Consequently, this method is effective in assessing the total amount of corrected surfaces. The results from this assessment are expected to correlate with solar incident angle, which is partly affected by solar elevation angle. In Sola *et al.* (2016), the interquartile range difference between a topographically corrected result and its original image could be as high as 10%.

### **3.8 Summary of topographic assessment methods**

A total of 11 papers from different journals were selected for review based on the seven assessment methods for topographic correction. The narrative literature methodology was used in this review paper to describe and synthesize the available literature on the topic and provide conclusions based on that evidence. A summary of the seven discussed assessment methods is presented in Table 2.

Table 2. Summary of topographic assessment methods.

Correction Methods	Reference	Short Description
Visual inspection	(Yin <i>et al.</i> 2018, Gao <i>et al.</i> 2016 and Shepherd <i>et al.</i> 2014)	It is fast and simple to use to detect an improvement without any computational analysis. However, the results cannot be quantified.
Incident angle correlation	(Yin <i>et al.</i> 2018 and Sola <i>et al.</i> 2016)	Topographic distortion is strongly related to solar incident angle. This method examines the correlation between an image and incident angle by examining the correlation between the data. Less correlation means that the topographic effect has been suppressed. Nevertheless, this method might not work in some areas physically affected by topography. After correction by using the PLC method, $R^2$ decreases from 0.089 to 0.015 for the red band of original images, indicating that the topographic effect is weakened (Yin <i>et al.</i> 2018).
Reduction of land cover variability	(Hantson and Chuvieco, 2011, Sola <i>et al.</i> 2016 and Gao <i>et al.</i> 2016)	This method requires prior knowledge on land cover distribution. Spectral radiance is collected from topographically corrected and uncorrected images for comparison. The variation within the same land cover is expected to reduce after the topographic correction. SD should decrease after successful correction, indicating that the impact of the topographic relief is reduced, with an average reduction of 10.7% (Gao <i>et al.</i> 2016).
Classification accuracy	(Sola <i>et al.</i> 2014, Hoshikawa and	Topographically corrected results are expected to have high classification results. This method compares the classification results before and

	Umezaki, 2014 and Tan <i>et al.</i> 2010)	after topographic correction. However, this method might have uncertainty in the classification procedure.
Calculation of the difference between north- and south-facing land covers	(Sola <i>et al.</i> 2016 Notarnicola <i>et al.</i> 2014 and Fan <i>et al.</i> 2014)	Ideally, topographic correction would reduce the difference between shaded and sunlit areas and increase the homogeneity. Sampling points from north- and south-facing surfaces are collected for the assessment. Most of the topographic correction methods used in their studies have achieved mean structural similarity index (MSSIM) values higher than 0.8 (Sola <i>et al.</i> 2016).
Presence of outliers	(Sola <i>et al.</i> 2016 and Balthazar <i>et al.</i> 2012)	A good topographic correction method should always return minimal outliers; hence, this method evaluates the proportion of statistical outliers to define the quality of a topographic correction method. Most of the topographic correction methods used in studies have achieved MSSIM values higher than 0.8 (Sola <i>et al.</i> 2016).
Intraclass interquartile range reduction	(Sola <i>et al.</i> 2016)	Similar to the reduction of land cover variability, this method uses the interquartile range to quantify the improvement after topographic correction. Nonetheless, the accuracy of this method may be affected by outliers. Most of the topographic correction methods used in studies have achieved MSSIM values higher than 0.8 (Sola <i>et al.</i> 2016).

---

#### 4.0 Case studies

A study conducted by Hantson and Chuvieco (2011), published in the International Journal of Applied Earth Observation and Geoinformation was used as a case study. They recommended the uses of empirical-statistical method for topographic correction, and they concluded that the empirical-statistical topographic correction method we have presented can correct topographic effects, providing satisfying results in the majority of cases (Figure 1).

Another study performed by Filgueurasi, et al. in 2017 published in the Journal of the Brazilian Association of Agricultural Engineering was as a second case study. They found that the C-correction method, is a modification of CC with the addition of factor C, which is adequate in accordance with qualitative and quantitative parameters and can correct the effects of topography on the values of radiation balance in the Edgárdia Experimental Farm as shown in Figure 2.

Based on the two case studies, we conclude that the empirical-statistical topographic correction method can be used to correct topographic effects and provide more satisfying results.

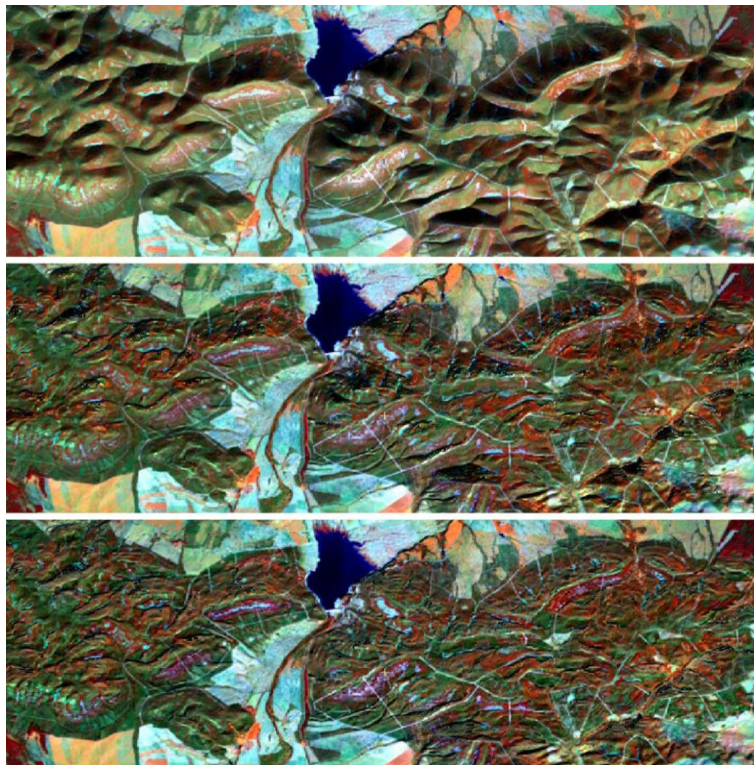


Fig.1. Comparison between the original image (up) and after c-correction (centre) and empiric–statistic correction (bottom), both with separation between land-cover. the image was taken at 24/11/1999 with a solar elevation angle of 28°.

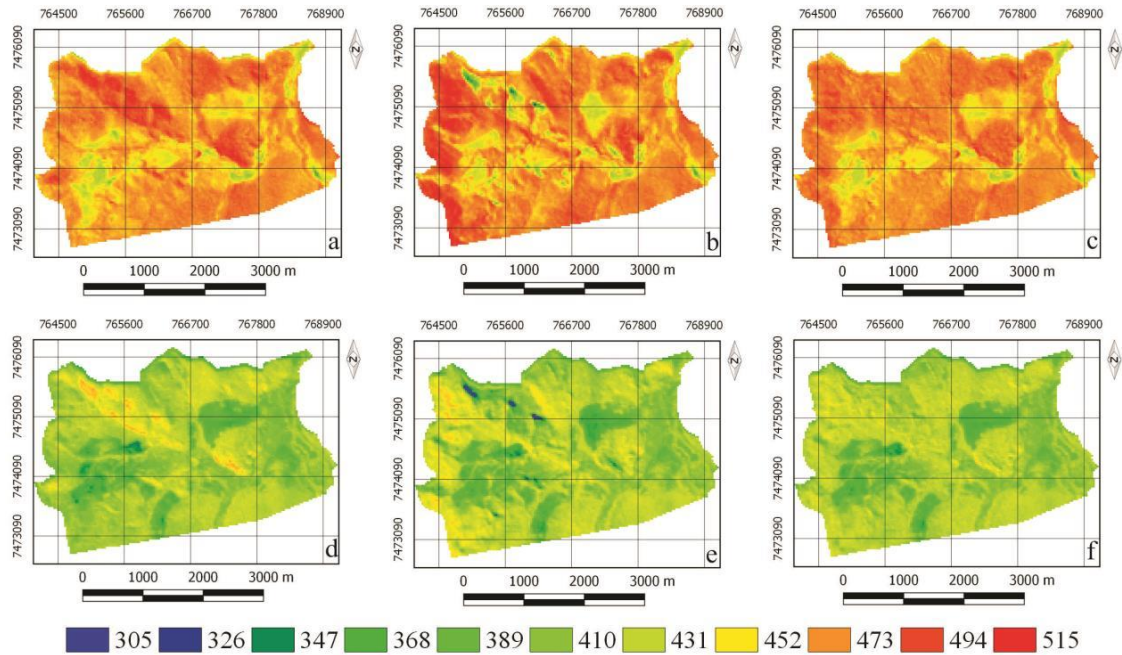


Fig. 2. Images of the radiation balance ( $W / m^2$ ), without topographic correction (a and d), with cosine correction (b and e) and C correction (c and f) referring to 09/11/1985 and 08/17/2005.

## 5.0 Summary

Topographic correction is a way to improve images topographically, which increases the accuracy of data but away from natural illumination. That is, a corrected image is supposed to be ideal illumination, which is impossible. Hence, real data free of topographical error are impossible. Based on the results from the review papers, it is evident that the topographic effect on satellite images can be reduced. The topographically corrected image improved in accuracy by reducing the spectral variation in the satellite image. This means that automation classification on rugged terrain is becoming a realistic proposition. Previously discussed assessment methods are merely for statistical assessment based on certain assumptions with no real data for comparison. These assessment methods are relatively applicable and quantitatively acceptable to a certain extent. Considerable topographic correction studies have been identified, which have applied various methods/algorithms to satellite imagery.

## Acknowledgements

All supports from Universiti Sains Malaysia (USM) and various parties are gratefully acknowledged. Authors acknowledge the Ministry of Higher Education (MOHE) for funding under the Fundamental Research Grant Scheme (FRGS) (Reference Code: FRGS/1/2021/STG08/USM/02/2).

## Reference

- Balthazar, V., V. Vanacker, and E. F. Lambin, 2012. Evaluation and parameterization of ATCOR3 topographic correction method for forest cover mapping in mountain areas. *International Journal of Applied Observation and Geoinformation* 18, 436–450.
- Bird, R. E., C. J. Riordan, and D. R. Myers, 1987. Investigation of a cloud-cover modification to SPCTRAL2, SERI's simple model for cloudless-sky, spectral solar irradiance (No. SERI/TR-215-3038). Solar Energy Research Inst., Golden, CO (USA).
- Bishop, M. and J. Colby, 2002. Anisotropic reflectance correction of SPOT-3 HRV imagery. *International Journal of Remote Sensing* 23, 2125–2131.
- Blesius, L. and F. Weirich, 2005. The use of the Minnaert correction for land-cover classification in mountainous terrain. *International Journal of Remote Sensing*, 26(17), pp.3831-3851.
- Brine, D.T., and M. Iqbal, 1983. Solar spectral diffuse irradiance under cloudless skies, *Solar Energy*, 30, 447-453.
- Civco, D. L., 1989. Topographic normalization of Landsat Thematic Mapper digital imagery. *Photogrammetric Engineering and Remote Sensing*, 55(9), pp.1303-1309.
- Coddington, O., J. L. Lean, P. Pilewskie, M. Snow, and D. Lindholm, 2016. A solar irradiance climate data record. *Bulletin of the American Meteorological Society*, 97(7), 1265-1282.
- Dong, C., Zhao, G., Meng, T., Li, B. and Peng, B., 2020, The Effect of Topographic Correction on Forest Tree Species Classification Accuracy, *Remote Sens.* 2020, 12(5), 787; <https://doi.org/10.3390/rs12050787>.
- Fan, Y., T. Koukal, and P. J. Weisberg, P2014. A sun–crown–sensor model and adapted C-correction logic for topographic correction of high resolution forest imagery. *ISPRS Journal of Photogrammetry and Remote Sensing*, 96, 94–105.
- Federico, S. and A. Palombo, 2022, Impact of Topographic Correction on PRISMA Sentinel 2 and Landsat 8 Images, *Remote Sensing*, 14, 3903. <https://doi.org/10.3390/rs14163903>

- Filgueiras, R., D. A. P. Nicolete, T. M. Carvalho, A. R. D. Cunha, and C. R. L. Zimback. 2017. Topographic aspects in the spatial and temporal dynamic of net radiation. *Journal of the Brazilian Association of Agricultural Engineering*. ISSN:1809-4430.  
Doi:<http://dx.doi.org/10.1590/1809-4430-Eng.Agric.v37n5p1028-1040/2017>.
- Fröhlich, C. and C. Wehrli, 1981. Spectral distribution of solar irradiance from 25000 nm to 250 nm. World Radiation Center, Davos, Switzerland.
- Gao, M., H. Gong, W. Zhao, B. Chen, Z. Chen, and M. Shi, 2016. An improved topographic correction model based on Minnaert. *GIScience & Remote Sensing*, 53(2), pp.247-264.
- Gao, M. L., W. J. Zhao, Z. N. Gong, H. L. Gong, Z. Chen, Z. and X. M. Tang, 2014. Topographic correction of ZY-3 satellite images and its effects on estimation of shrub leaf biomass in mountainous areas. *Remote Sensing* 6, 2745–2764.
- Gregg, W. W. and K. L. Carder, 1990. A Simple Spectral Solar Irradiance Model for Cloudless Maritime Atmospheres. *Journal of Limnology and Oceanography*, 1990, Vol.35, No.8: 1657-1675.
- Gao, Y and W. Zhang, 2009. A simple empirical topographic correction method for ETM+ imagery, *International Journal of Remote Sensing*, 30(9), 2259-2275,  
<https://doi.org/10.1080/01431160802549336>
- Hantson, S. and E. Chuvieco, 2011. Evaluation of different topographic correction methods for Landsat imagery. *International Journal of Applied Earth Observation and Geoinformation*, 13(5), pp.691-700.
- Hart, C. and M. Gartley, 2010. Incorporation of cloud radiance effects into hyperspectral target detection. In *2010 IEEE International Geoscience and Remote Sensing Symposium* (pp. 1617-1620). IEEE.
- Hoshikawa, K. and M. Umezaki, 2014. Effects of terrain-induced shade removal using global DEM data sets on land-cover classification. *International Journal of Remote Sensing*, 35, 1331–1355.
- Huang, H., P. Gong, N. Clinton, and F. Hui, 2008. Reduction of atmospheric and topographic effect on Landsat TM data for forest classification. *International Journal of Remote Sensing*, 29(19), pp.5623-5642.
- Hu, R., G. Yan, F. Nerry, Y. Liu, Y., Jiang, S. Wang, Y. Chen, X. Mu, W. Zhang, and D. Xie, 2018. Using airborne laser scanner and path length distribution model to quantify clumping effect

- and estimate leaf area index. *IEEE Transactions on Geoscience and Remote Sensing*, 56(6), pp.3196-3209.
- Kaskaoutis, D. G. and H. D. Kambezidis, 2008. The role of aerosol models of the SMARTS code in predicting the spectral direct-beam irradiance in an urban area. *Renewable Energy*, 33(7), pp.1532-1543.
- Leckner, B., 1978. The spectral distribution of solar radiation at the earth's surface—elements of a model. *Solar Energy*, Vol. 20. pp. 143-150.
- Luisa, E. M., B. Frédéric, and W. Marie, 2008. Slope correction for LAI estimation from gap fraction measurements. *Agricultural and forest meteorology*, 148(10), pp.1553-1562.
- Minnaert, M., 1941. The reciprocity principle in lunar photometry. *The Astrophysical Journal*, 93, pp.403-410.
- Mishra, V.D., J.K. Sharma and R. Khanna, (2017) Review of topographic analysis methods for the western Himalaya using AWiFS and MODIS satellite imagery, *Annals of Glaciology*, 51(54).
- Notarnicola, C., M. Callegari, L. De Gregorio, R. Sonnenschein, R., Remelgado, and B. entura, 2014. A novel topographic correction for high and medium resolution images by using combined solar radiation. *Proceedings, IGARSS 2014 symposium*, Québec, Canada, pp. 1053–1056.
- Pandya, M. R., D. B. Shah, H. J. Trivedi, and S. Panigrahy, 2011. Simulation of at-sensor radiance over land for proposed thermal channels of Imager payload onboard INSAT-3D satellite using MODTRAN model. *Journal of earth system science*, 120(1), pp.19-25.
- Qiu, S., Y. Lin, R. Shang, J. Zhang, L. Ma, and Z. Zhu, 2019. Making Landsat Time Series Consistent: Evaluating and Improving Landsat Analysis Ready Data. *Remote Sensing*, 11(1), p.51.
- Richter, R., T. Kellenberger, and H. Kaufmann, 2009. Comparison of topographic correction methods. *Remote Sensing*, 1(3), pp.184-196.
- Shepherd, J. D. and J. R. Dymond, 2003. Correcting satellite imagery for the variance of reflectance and illumination with topography, *International Journal Remote Sensing*, 2003, vol.24, no.17,3503-3514.

- Shepherd, J. D., J. R. Dymond, S. Gillingham, and P. Bunting, 2014. Accurate registration of optical satellite imagery with elevation models for topographic correction. *Remote Sensing Letters*, 5, 637–641.
- Sola, I., G. A. Maria, and A. M. Jesus. 2016. Multi-criteria evaluation of topographic correction methods. *Remote sensing of environment*, 184 (2016) 247-262.
- Sola, I., G. A. Maria, A. M. Jesus, and L. T. Jose, 2014. Synthetic images for evaluating topographic correction algorithm, *IEEE Transaction on geoscience and remote sensing*, vol.52, no.3, March 2014.
- Soenen, S. A., D. R. Peddle, and C. A. Coburn, 2005. SCS+ C: A modified Sun-canopy-sensor topographic correction in forested terrain. *IEEE Transactions on geoscience and remote sensing*, 43(9), pp.2148-2159.
- Tan, K. C., H. S. Lim, M. Z. MatJafri, and K. Abdullah, 2010. Landsat data to evaluate urban expansion and determine land use/land cover changes in Penang Island, Malaysia. *Environmental Earth Sciences*, 60(7), pp.1509-1521.
- Teillet, P. M., B. Guindon, and D. G. Goodenough, 1982. On the slope-aspect correction of multispectral scanner data. *Canadian Journal of Remote Sensing*, 8(2), pp.84-106.
- Thompson, D. R., L. Guanter, A. Berk, B. C. Gao, R. Richter, D. Schlöpfer, and K. J. Thome, 2018. Retrieval of atmospheric parameters and surface reflectance from visible and shortwave infrared imaging spectroscopy data. *Surveys in Geophysics*, 40(3), pp.333-360.
- Vanonckelen, S., S. Lhermitte, V. Balthazar and A. V. Rompaey, (2014), Performance of atmospheric and topographic correction methods on Landsat imagery in mountain areas, *International Journal of Remote Sensing*, 35(13), pg 4952-4972.
- Wallach, H. and D. N. O'connell, 1953. The kinetic depth effect. *Journal of experimental psychology*, 45(4), p.205.
- Yan, G., R. Hu, Y. Wang, H. Ren, W. Song, J. Qi, and L. Chen, 2016. Scale effect in indirect measurement of leaf area index. *IEEE Transactions on Geoscience and Remote Sensing*, 54(6), pp.3475-3484.
- Yin, G., A. Li, S. Wu, W. Fan, Y. Zeng, K. Yan, B. Xu, J. Li, and Q. Liu, 2018. PLC: A simple and semi-physical topographic correction method for vegetation canopies based on path length correction. *Remote Sensing of Environment*, 215, pp.184-198.

Yin, H., Tan, B., Frantz, D. and Radeloff, V. C., 2022, Integrated topographic corrections improve forest mapping using Landsat imagery Author links open overlay panel, *International Journal of Applied Earth Observation and Geoinformation*, 108, 102716.